S-NitrosoAcetylPenicillamine Upregulates Metabolic and Differentiated Function in Hepatocyte-like Cells derived from Embryonic Stem Cells

Journal:	*Stem Cells*
Manuscript ID:	SC-07-1119
Manuscript Type:	Original Research
Date Submitted by the Author:	29-Dec-2007
Complete List of Authors:	Sharma, Nripen; Rutgers The State University of New Jersey, Chemical and Biochemical Engineering Wallenstein, Eric; Rutgers The State University of New Jersey, Biomedical Engineering Novik, Eric; Rutgers The State; Rutgers The State University of New Jersey, Biomedical Engineering Maguire, Timothy; Rutgers The State University of New Jersey, Biomedical Engineering Schloss, Rene; Rutgers The State University of New Jersey, Biomedical Engineering Yarmush, Martin; Rutgers The State University of New Jersey, Biomedical Engineering
Keywords:	Embryonic stem cells, In vitro differentiation, Hepatocyte-like Cells, S-NitrosoAcetylPenicillamine

Running Head of Title: Hepatic Differentiation of Embryonic Stem Cells

S-NitrosoAcetylPenicillamine Upregulates Metabolic and Differentiated Function in Hepatocyte-like Cells Derived from Embryonic Stem Cells

N. S. Sharma [1], E. J. Wallenstein [2], E. Novik [2], T. Maguire [2], R. Schloss [2], M. L. Yarmush [2]

1. Department of Chemical & Biochemical Engineering, Rutgers University, 98 Brett Road, Piscataway, NJ 08854

2. Department of Biomedical Engineering, Rutgers University, 617 Bowser Road, Piscataway, NJ 08854

Correspondence:

Martin L. Yarmush

599 Taylor Road

Piscataway, NJ 08854

Telephone: (732) 445-4500

Fax: (732)445-3753

Email: KMA@soemail.rutgers.edu

Contract Grant Sponsor: National Institute of Health, Hepatic Tissue Engineering Grant

Contract Grant Number: R01DK43371

Keywords: Embryonic Stem Cells, In Vitro Differentiation, Hepatocyte-like Cells, S-NitrosoAcetylPenicillamine.

INTRODUCTION

The liver plays a significant role in coordinating whole-body metabolism. Hepatocytes constitute approximately 70 % of the cellular population of the liver and perform major metabolic functions such as plasma protein synthesis and transport, xenobiotic metabolism, glucose homeostasis, urea synthesis and ketogenesis (1). The generation of functionally and energetically mature hepatocyte-like cells may provide an excellent cell source for diverse applications. From a clinical standpoint, it is known that in cases of irreversible liver failure such as cirrhosis and fulminant hepatic failure, an alternative functional hepatic device to sustain life is vital. While the extracorporeal Bio-Artificial Liver (BAL) is a promising technology for the treatment of liver failure [2, 3], the difficulty in *in vitro* culture of hepatocytes and scarcity of cells is an impending problem. From a diagnostic stand point, hepatocytes are a useful cell source for *in vitro* drug screening and toxicity studies. The generation of fully functional hepatocyte-like cells from a renewable cell source can provide an unlimited resource for clinical and diagnostic applications.

Embryonic Stem (ES) cells are highly proliferative, pluripotent cells isolated from the Inner Cell Mass (ICM) of the embryo [4]. These cells, when cultured *in vitro* under suitable conditions, proliferate indefinitely and have the potential to generate almost any cell type in the body under controlled differentiation regimens, including hepatocytes [5-8]. Currently the two major problems with obtaining hepatocytes from ES cells are (a) generation of a mixed population and (b) incomplete functional differentiation into the hepatocyte lineage.

In this regard, we have previously developed a directed differentiation system to obtain an enriched population of hepatocyte-like cells using Na-butyrate treatment [8]. These cells have been shown to possess hepatocyte-specific characteristics. In addition, since hepatocytes are biochemically active and perform complex metabolic functions in association with high aerobic metabolism for mitochondrial ATP generation, we performed a metabolic analysis of the hepatocyte-like cells to identify its metabolic and functional phenotype. We have shown that Na-butyrate treated hepatocyte-like cells have a glycolytic energetic phenotype that is similar to fetal hepatocytes/mouse hepatoma cells. Specifically, these cells have lower urea and albumin secretion rates as compared to mature hepatocytes [9].

It is well known that nitric oxide triggers mitochondrial biogenesis in a variety of mammalian cells [10-12]. Both NO and NOS isoforms have been shown to induce differentiation of nerve cells, tumor cells and cardiomyocytes [13-15]. The phenomenon of mitochondrial biogenesis involves the increase in mitochondrial mass, activity and the induction of respiratory enzymes implicated in oxidative metabolism. The long term process of mitochondrial proliferation involving increase in mitochondrial number and mass is apparent throughout the developmental

process. The short term process, mitochondrial differentiation is an hour long process immediately after birth and results in induction of mitochondrial metabolic enzymes. This process has been known to be present in liver developmental processes. Immediately after birth, there is an increase in liver metabolic enzyme activities concomitant with increased oxygen consumption rates and higher biochemical function.

In the present studies, we have investigated the phenomena of mitochondrial biogenesis during the hepatic differentiation process in cell populations as a methodology to augment differentiated function in ES cell derived hepatocyte-like cells.

In this regard, we have utilized S-NitrosoAcetylPenicillamine (SNAP), a nitric oxide donor to increase mitochondrial development in Na-butyrate treated hepatocyte-like cells and have shown that an increase in mitochondrial mass and activity is instrumental in increasing hepatic differentiated function.

MATERIALS AND METHODS

ES Cell Culture

The ES-D3 cell line (ATCC, Manassas, VA) was maintained in an undifferentiated state in T-75 gelatin-coated dishes (BD-Biosciences, Bedford, MA) in Knockout Dulbecco's Modified Eagles Medium (Gibco, Grand Island, NY) containing 15 % knockout serum (Gibco, Cat # 10828-028), 4 mM L-glutamine (Gibco), 100 U/ml penicillin (Gibco), 100 U/ml streptomycin (Gibco), 10 µg/ml gentamicin (Gibco), 1000 U/ml ESGRO (Chemicon, Temecula, CA) and 0.1mM 2-mercaptoethanol (Sigma-Aldrich, St. Louis, MO). To maintain cells in the undifferentiated state, media was changed every two days until plates were confluent. Cells were dissociated using trypsin EDTA (Gibco, Cat # 25200-056) and passaged by further replating. Only cells between passages 10-20 were used for differentiation. All cell cultures were incubated at 37°C in a humidified 5% CO_2 incubator.

HEPA Cell Culture

Mouse hepatoma cells (Hepa 1-6 cells) (ATCC) were cultured in polystyrene T-75 flasks in Dulbecco's Modified Eagle's Medium (DMEM) (Gibco, Cat # 10313-021) supplemented with 10 % Fetal Bovine Serum (Gibco, Cat # 26140-079), 4 mM L-glutamine (Gibco) and 100 U/ml Penicillin/Streptomycin (Gibco). Cell media was replaced every two days.

Differentiation Using Sodium Butyrate

On day 0 of differentiation, ES cells were plated at a density of 10^5 cells/well in 0.1 % gelatin coated six well plates in Iscove's Modified Dulbecco's medium (IMDM) (Gibco, Cat # 31980-030) containing 20 % fetal bovine serum (Gibco), 4 mM L-glutamine (Gibco), 100 U/ml penicillin, 100 U/ml streptomycin (Gibco) and 10 µg/ml gentamicin (Gibco). Gelatin solution (0.1 %) was prepared by dissolving 0.5 gm of porcine gelatin (Sigma-Aldrich, Cat # G-2500) in 500 ml of Phosphate Buffered Saline (PBS) (Gibco, Cat # 20012-027) with gentle heating. To coat plates with gelatin, 2 ml of 0.1 % gelatin solution was added to each well of a polystyrene tissue culture treated plate. The plates were incubated for 2 hrs following which the gelatin solution was aspirated. The plates were washed once with PBS and then 2.5 ml of IMDM was added followed by 10^5cells/well. Cells were exposed to 1 % dimethylsulfoxide (DMSO) (Sigma-Aldrich) for the next 4 days followed by exposure to 2.5 mM Na-butyrate (Sigma Aldrich, Cat # B5887) for 6 days. Media was replaced daily.

For hepatic functional assessment, cells were removed from the primary culture dish and replated on day 11 of differentiation in polystyrene 12 well plates at a density of 10^5cells/well.

Induction of Mitochondrial Development

On day 12, 24 hrs after replating, cells were exposed to IMDM supplemented with different concentrations of SNAP for three days. Serial dilutions of SNAP were prepared by dissolving different amounts of SNAP in a predetermined volume of DMSO concentration adjusted to 5 % of total media content to prevent DMSO effects. Day 13 and day 15 were chosen as analysis days and metabolic analysis was performed on these days. In parallel, hepatic functional characteristics viz. intracellular albumin content, urea and albumin secretion rate and cytochrome p450 7α1 (cyp7a1) promoter activity were evaluated.

Cell Number

Cultures were treated with PBS followed by incubation with trypsin-EDTA for 3 mins. Dissociated cells from each condition were suspended in differentiation media and centrifuged at 1000 rpm for 5 mins. The media with trypsin was decanted and cells were re-suspended in fresh media. Cells were counted using a hemocytometer using 1% trypan blue exclusion. In primary culture, exposure to DMSO resulted in about 3.10^6 cells/ well on day 5. On day 8, cell number reduced to 10^6cells/well and remained at that on day 11. After replating on day 11, cell number

remained constant after 48 hrs of replating for all conditions. On day 15 of differentiation, there was a linear decrease in viable cells with increase in SNAP concentration.

Urea Analysis

Media samples were collected directly from cell cultures on days 13 and 15 post differentiation for the different experimental conditions and stored at -20°C for subsequent analysis for urea content. Urea synthesis was assayed using a commercially available kit (StanBio, Boerne, Texas, Cat # 2050-450). Urea enzyme reagent (100 µl) was added to each well of a 96 well plate followed by addition of 10 µl of standards/samples to the enzyme reagent. The plates were centrifuged at 1000 rpm for 1 min and then placed in a water bath at 37°C for 5 minutes. Urea color reagent (100 µl) was then added to each well followed by centrifugation and water-bath treatment. Absorbance readings were obtained using a Biorad (Hercules, CA) Model 680 plate reader with a 585nm emission filter. A standard curve was generated by creating serial dilutions of a urea standard from 0-300 µg/ml and a linear fit of the standards was used to determine the urea concentration in each sample.

Albumin ELISA Assay

In order to detect secreted albumin within the media supernatants obtained on each of the analysis days, we used a commercially available mouse albumin ELISA kit (Bethyl Laboratories, #E90-134). A standard curve was generated by creating serial dilutions of an albumin standard from 7.8-10,000 ng/ml. Absorbance readings were obtained using a Biorad (Hercules, CA) Model 680 plate reader with a 490 nm emission filter. Albumin values were normalized to the cell number recorded on the day of media sample collection.

In Situ Indirect Immunofluorescent for Intracellular Albumin

On evaluation days as indicated for the urea assay, cells were washed with PBS and fixed in 4% paraformaldehyde (Sigma-Aldrich) in PBS for 15 minutes at room temperature. The cells were washed twice in cold PBS and then twice in cold saponine/PBS (SAP) membrane permeabilization buffer containing 1% bovine serum albumin (BSA) (Sigma-Aldrich, Cat # A7906), 0.5% saponine (Sigma-Aldrich, Cat # 54521) and 0.1% sodium azide (Sigma-Aldrich, Cat # 58032). The cells were subsequently incubated for 30 minutes at 4°C in a SAP solution containing rabbit anti-mouse albumin antibody (150 µg/ml) (MP Biomedicals, Irvine, CA), or Normal Rabbit Serum (NRS)

(150 μg/ml) (MP Biomedicals) as an isotype control, washed twice for 10 min in cold SAP buffer, and then treated for 30 minutes at 4°C with the secondary antibody, FITC-conjugated donkey anti-rabbit, diluted 1:500 (Jackson Immuno Labs, Westgrove, PA). Cells were then washed once with cold SAP buffer and once with cold PBS. Fluorescent images were acquired with an Olympus IX70 microscope and Olympus digital camera using an excitation filter of 515 nm. Image quantification was conducted using Olympus Microsuite. To generate intensity values for each of the samples, 15-20 cells were randomly chosen from each image taken (3 images per well per experiment). The average intensity value for these cells was measured in the NRS fluorescent (control) case and was subtracted from each of 15-20 randomly selected cells in the test (anti-albumin) case to quantify the number of albumin positive cells per image. This was done in triplicate experiments yielding a total of 135-180 cells per condition.

Cloning of the Cytochrome p450 7α1 (cyp7a1) Promoter Driven pDsRedExpress1 Vectors

The pDsRedExpress1 plasmid vector was attained from BD Biosciences Clontech (Mountain View, CA). The cytochrome p450 7α1 (cyp7a1) vector was donated in the form of a PGL3-Promoter vector from Dr. Gregorio Gil (Virginia Commonwealth University, Richmond, VA). The promoter regulatory elements were each excised at a blunt and a sticky end and inserted via ligation into respective blunt and sticky sites in the parent pDsRedExpress1 vector. Correct insertion of the regulatory elements into the pDsRedExpress1 vector was confirmed by screening bacterial clones via test transfections in mouse Hepa 1-6 cells and through DNA sequencing. The vector is hereby referred to as pcyp7a1-dsRedExpress1. An additional vector, pDsRed2-C1, driven by the constitutive cytomegalovirus, was used as a control for positive transfection of different cell types.

Transient Transfection of Liver-Specific Vectors into Differentiated Stem Cells

On day 13 of differentiation, the liver-specific expression vector pcyp7a1-dsRedExpress1, along with the constitutive pDsRed2-C1 plasmid, was transiently transfected into the distinct differentiated stem cell populations. A control plate of murine Hepa 1-6 cells was used to assess transient transfection efficiency. Following 48 h, red fluorescent activity was detected via flow cytometry and imaged for fluorescent activity using a computer-interfaced inverted Olympus IX70 microscope.

Extracellular Metabolite Measurements

Supernatants (1 ml) were collected in triplicate for differentiated cells in secondary culture on days 13 and 15 of differentiation and tested using a Bioprofile Bioanalyzer 400 (Nova Biomedical, Waltham, MA) for metabolite measurements of glucose, lactate, glutamine, glutamate and ammonia.

In order to confirm that replating doesn't change the metabolic properties in control cell populations, mouse hepatoma cells were cultured for 5 days in six well plates. Media was replaced daily and on the 5^{th} day, supernatants were collected for lactate measurements. Cells were trypsinized, resuspended and 10^5 cells were replated in each well of a 12 well plate and media was changed after 24 hrs. After 48 hrs, we found that mouse hepatoma cells have a similar lactate production rate in both primary culture (6.6±0.5 μmol/million cells/day) and replated conditions (6.3± 0.7 μmol/million cells/day).

On each day of analysis, base media glucose, lactate, glutamine, glutamate and ammonia measurements were measured and the mean values were subtracted from the test values to obtain uptake or production. Cells were counted for each condition to get the final consumption or production rate.

Mitochondrial Mass

On each analysis day of secondary culture, cells from different experimental conditions in each well of a polystyrene 48 well plate were washed with PBS and exposed to 10 μM N-Acridine Orange dye (NAO) (Molecular Probes, Eugene, MO) for 10 minutes at room temperature. Cells were washed twice in PBS and then exposed to PBS. Experimental analysis was performed with the FL3 filter using the Olympus IX70 microscope and image analysis was performed using Microsuite software. On each day of analysis, undifferentiated ES cells and mouse hepatoma cells were stained as negative and positive controls respectively. To generate intensity values for each of the samples, 15-20 cells were randomly chosen from each image taken (3 images per well per experiment). The average intensity value for these cells was measured in the particular condition and subtracted from each of 15-20 randomly selected cells in the undifferentiated ES cell fluorescent case to quantify the number of NAO positive cells per image. This was done in triplicate experiments yielding a total of 135-180 cells per condition.

Mitochondrial Activity ($\Delta\psi$)

On analysis days, cells in each well were washed with PBS and then exposed to 30 μM JC-1 dye (Molecular Probes) for 30 minutes at 37°C, 10 % CO_2 at a density of $2.5.10^4$ cells/ml in polystyrene 48 well plates. Cells were washed twice in PBS. Since JC-1 dye forms a monomer at low mitochondrial potential with a green fluorescence while at high mitochondrial membrane potential, it aggregates and exhibits an orange fluorescence, image acquisition was performed with the FL2 and FL1 filter using the Olympus microscope and image analysis was performed using the Microsuite software. On each day of analysis, undifferentiated ES cells and mouse hepatoma cells were stained as negative and positive controls respectively. To generate intensity values for each of the samples, 15-20 cells were randomly chosen from each image taken (3 images per well per experiment). The average intensity value for these cells was measured in the particular condition and subtracted from each of 15-20 randomly selected cells in the undifferentiated ES cell fluorescent case to quantify the number of JC-1 positive cells per image. This was done in triplicate experiments yielding a total of 135-180 cells per condition.

Statistical Analysis

Each data point represents the mean of three experiments (each with three biological replicates), and the error bars represent the standard error of the mean. Statistical significance was determined using the student t-test for unpaired data. Differences were considered significant when the probability was less than or equal to 0.05.

RESULTS

Establishment of System for Metabolic Maturation

We have previously developed a Na-butyrate treated ES cell differentiation system to generate an enriched population of hepatocyte-like cells [8]. In addition, we performed a metabolic analysis of the populations to characterize the energy status of the cells. We have shown that hepatocyte-like cells have reduced function with the expression of a glycolytic phenotype similar to immature hepatocytes. Thus, we employed a procedure to alter the energetic profile of the cells towards a mature hepatocyte phenotype in order to upregulate hepatocyte-specific function.

On day 11 of differentiation, 2.5 mM Na-butyrate treated ES cells were replated in polystyrene 12 well plates. On Day 12, cells were exposed to 0, 50, 100, 250 or 500 μM SNAP for 3 additional days. Functional and metabolic analyses were performed on days 13 and 15 of differentiation.

Energetics of Hepatic Differentiation

Hepatocyte-like cells have been shown to have an energetic profile similar to fetal hepatocytes/ mouse hepatoma cells [8] and we investigated the effects of SNAP on the energy status of these cells. Since hepatic function is tightly linked to intermediary metabolism, we hypothesized that an increase in oxidative metabolism can lead to increased hepatic function.

Glucose and Lactate metabolism

Primary hepatocytes have higher glucose consumption rates as compared to the fetal phenotype. We investigated this phenomena in SNAP treated hepatocyte-like cells as shown in Figure 1. "No SNAP" and "DMSO" conditions correspond to Na-butyrate treated ES cells exposed to differentiation media only and media supplementation with DMSO only in secondary culture respectively. Figure 1A shows that hepatocyte-like cells have comparable glucose consumption rates on day 13 independent of SNAP exposure. On the other hand, there was a significant decrease in the consumption rate on day 15 for the "No SNAP" condition (~ 2 fold) whereas there was a significant increase in glucose consumption rate for 250 μM (~ 1.5 fold) and 500 μM SNAP (~ 2 fold) treated hepatocyte-like cells as compared to day 13 of differentiation.

For lactate production rate, as shown in Figure 1B, irrespective of the SNAP concentration, day 13 SNAP treated cells showed a similar but higher lactate production rate as compared to the "No SNAP" condition. Also, there was no significant change in lactate production on day 15 of differentiation for both 250 μM and 500 μM SNAP treated cells as compared to day 13 of differentiation while the lactate production rate was lower for all other conditions on day 15 as compared to day 13 of differentiation.

Thus, exposure to 250 μM and 500 μM SNAP resulted in higher glucose consumption rate and lactate production rates for hepatocyte-like cells on day 15 of differentiation. The next step was to investigate the effect of SNAP on mitochondrial parameters, viz. mitochondrial mass and activity.

Mitochondrial Mass and Activity

As shown in Figure 2A, on day 15, microscopic evaluation indicated that the mitochondrial activity was highest for 500 μM SNAP treated cells. Similarly, the mitochondrial mass was highest for 500 μM SNAP treated cells. Additionally, we quantified the percentage of cells with higher mitochondrial mass (Figure 2B) and activity (Figure 2C). As shown, 500 μM SNAP resulted in about ~ 80 % of cells with a higher mitochondrial mass and activity as compared to the "No SNAP' condition on day 15 of differentiation. For 250 μM SNAP treated cells, increase in percentage of cells with higher mitochondrial activity was not concomitant with increase in percentage of NAO positive cells.

Evaluation of Hepatic Function

The next step was to assess the effects of different concentrations of SNAP on hepatocyte-specific function. Our hypothesis is that an induction of mitochondrial development in hepatocyte-like cells is associated with an increase in cellular function. As a result, we assessed two extracellular functions, urea and albumin secretion and two intracellular markers viz. the presence of intracellular albumin and cytochrome P450 7A1 promoter activity to identify if a particular SNAP concentration was effective in increasing function.

Urea and albumin secretion

As shown in Figure 3A, urea synthesis rate was similar for different experimental conditions on day 13 of differentiation. However, on day 15, there was an increase in secretion rates for 250 μM and 500 μM SNAP treated hepatocyte-like cells. This increase was about 2 fold higher as compared to Na-butyrate treated hepatocyte-like cells ("No SNAP" condition on day 13 of differentiation). Figure 3B showed a similar trend for albumin secretion rate on day 13 of differentiation. However, while there was a decrease in albumin secretion on day 15 for the "No SNAP" condition, there was a stabilization of function in the presence of 250 μM or 500 μM SNAP.

The mitochondrial and functional assessments indicate that 500 μM SNAP treatment resulted in increased mitochondrial mass and activity and higher glucose consumption rates on day 15 of differentiation. More importantly, the alteration in metabolic characteristics was concomitant with increase in urea and albumin secretion rates.

Intracellular Albumin and cyp 7A1 Promoter Activity

While urea and albumin secretion are representative of an average population, these characteristics do not provide information about the intracellular characteristics within the cell population. As a result, we performed an immunofluorescent assay to test for intracellular albumin. As shown in Figure 4A, there was a drastic difference in intracellular albumin content between the different conditions on day 15 of differentiation. It was evident from the microscopic analysis that 500 μM SNAP treated hepatocyte-like cells showed a higher intracellular albumin intensity as compared to any other experimental condition. Figure 4B shows the percentage of cells positive for albumin under different experimental conditions. As shown, 500 μM SNAP treatment resulted in ~ 80% albumin positive cells on day 15 of differentiation. This implied that 500 μM SNAP treatment resulted in the generation of an enriched population of albumin positive cells that secrete albumin, urea and possess improved metabolic characteristics closer to the mature hepatic phenotype. On the other hand, 250 μM SNAP treatment resulted in a heterogeneous population (~65 % albumin positive cells) while there are fewer positive cells in the other conditions. In the absence of SNAP, percentage of albumin expressing cells decreased to 35 % by day 15 post-differentiation.

In order to confirm the presence of a hepatocyte-specific marker, cyp7A1 promoter activity was determined in the different conditions on day 15 of differentiation. Cyp7A1 (cholesterol 7α-hydroxylase) is a rate-limiting enzyme implicated in cholesterol metabolism in the liver [16]. As shown in Figure 5, the highest promoter activity was observed in 500 μM SNAP treated cells. Thus, even though the metabolic secretion rates and mitochondrial activity were similar for 250 μM and 500 μM SNAP exposure, 500 μM SNAP treatment was the only experimental condition that resulted in the selection of an enriched population of hepatocyte-like cells with increased mitochondrial and hepatic functionality including cyp7A1 promoter activity.

DISCUSSION

We have previously established a directed differentiation system wherein Na-butyrate treated ES cells generates an enriched population of hepatocyte-like cells [8]. A metabolic analysis of the population showed that the hepatocyte-like cells have a glycolytic energy status similar to fetal hepatocytes with incomplete metabolic and quantitative hepatic differentiated function. In this context, we have investigated the effects of SNAP, a nitric oxide donor molecule implicated in mitochondrial development on Na-butyrate treated hepatocyte-like cells derived from ES cells.

From a mechanistic standpoint, numerous studies have identified PGC-1α, a downstream target of SNAP as the key regulator of energy metabolism. PGC-1α is a transcriptional co-activator and is implicated in the switch from glycolytic (anaerobic) to oxidative phosphorylation (aerobic) metabolism for ATP synthesis. PGC-1α docks on specific transcription factors increasing the affinity of the transcription complex to coactivators possessing histone acetyltransferase (HAT) activity. The end result is acetylation of histone proteins that increases the accessibility of DNA to the transcription complex [17]. Although there are three members of the PGC-1 family (PGC-1α, PGC-1β, and PGC-1α related coactivator [18]), PGC-1α has been gaining interest since it is a powerful regulator of energy metabolism under conditions of both health and disease [19].

While the effects of NO and NOS isoforms in association with PGC-1α is well known in primary and transformed cell lines, the utilization of these molecules in cellular differentiation is less studied. The effect of SNAP, a nitric oxide donor, has been investigated in liver cell systems [20-25]. *In vivo* liver developmental studies have been shown to involve complex set of events related to mitochondrial development. This phenomenon, known as mitochondrial biogenesis has been well studied due to the enormous biochemical capacity of hepatocytes, the primary functional cells of the liver. These studies have shown that PGC-1α is implicated in hepatic mitochondrial biogenesis wherein an increase in mitochondrial mass, number and activity is observed. This increase, which occurs immediately after birth, is associated with an increase in oxygen consumption, induction of mitochondrial respiratory enzymes and increased/induced terminally differentiated function. It has been shown that fetal hepatocytes have a more compromised (glycolytic) energy state and lower functional secretion rates as compared to highly functional mature hepatocytes with complex, functional mitochondria. The embryonic liver is primarily responsible for hematopoiesis during fetal development and undergoes many metabolic changes just before and after birth [26]. The ability to activate gluconeogenesis, beta-oxidation of fatty acids and ketogenesis are all characteristics of mature hepatocytes, which are functionally different from embryonic liver cells. In summary, the identification of the mechanism of NO induction of PGC-1α in mitochondrial biogenesis holds tremendous promise for applications in hepatocyte development from ES cells.

Many studies have shown the influence of NO inducers on mitochondrial development. These studies have been implicated in diverse cell lines such as Hela cells, brown adipocytes, 3T3-L1 and U937 cells [11]. In addition, SNAP, a nitric oxide donor had been successfully shown to induce cardiomyogenesis in ES cells [27]. 250 μM SNAP induced cardiomyogenesis in embryoid body aggregates based on the hanging drop culture protocol. In the

experimental set-up, ES cells were exposed to the molecule at earlier time points which differed from our experimental analysis wherein SNAP was supplemented after Na-butyrate treatment. It is well documented that SNAP, though shown to increase oxygen consumption [28] and mitochondrial development in hepatocytes leads to cell death [29]. While the exact mechanism for this phenomenon in our system is unknown, we observed a decrease in cell number at higher SNAP concentrations (data not shown).

Figure 1 shows the metabolic assessment of SNAP treated cells. As shown, SNAP increased glucose clearance rates at higher concentrations on day 15 of differentiation. This observation is known to be prevalent in mature hepatocytes to consume higher glucose rates than fetal hepatocytes for performing metabolic functions. It is worth mentioning that while glucose consumption rates were highest on day 15 for 250 μM and 500 μM treated hepatocyte-like cells, the lactate production rates were similar implying that SNAP increased glucose metabolism concomitant with increased mitochondrial mass and activity (Figure 2A) that is indicative of mitochondrial biogenesis. This increase was associated with an increased percentage in mitochondrial mass (Figure 2B) and activity (Figure 2C) for 500 μM SNAP treated cells on day 15 of differentiation. These increased mitochondrial parameters were shown in various mammalian cell lines after 3-4 days of SNAP treatment [28]. From a concentration standpoint, while 100 μM SNAP were used for different cell lines [11], 250 μM SNAP was shown to induce ES-cardiomyocyte differentiation [27]. In our population, we showed highest mitochondrial mass and activity in 500 μM SNAP treated cells. Beyond this concentration, we observed a significant decrease in cell viability and loss of mitochondrial function (data not shown).

Figure 3 showed the functional evaluation of hepatic characteristics after SNAP exposure. It is noteworthy that both 250 and 500uM SNAP exposure increased urea secretion by ~2 fold on day 15 of differentiation. This was associated with a stabilization of albumin secretion for the two conditions (Figure 3B). Since 250 μM SNAP induced mitochondrial and cardiomyogenic differentiation in ES cells, we performed an intracellular assessment of albumin to confirm the percentage homogeneity of cells. The "No SNAP" condition cells showed reduced intracellular albumin over time which was consistent with albumin secretion rates. As shown in Figure 4, while the 250 μM SNAP treated cells revealed a mixed population indicative of different lineages, the 500 μM SNAP treatment resulted in a relatively higher enriched population of albumin positive cells (~ 80%, Figure 4B). In addition to albumin, we performed an intracellular cyp7A1 promoter activity analysis, a hepatocyte specific enzyme implicated in cholesterol metabolism [30, 31]. As shown in Figure 5, this marker has highest activity in 500 μM

SNAP treated cells implying this was the best condition for generating a homogenous population of albumin positive cells with higher urea, albumin secretion rates and cyp7A1 promoter activity as compared to Na-butyrate treated hepatocyte-like cells.

CONCLUSION

We utilized experimental techniques to improve function of hepatocyte-like cells using the concept of mitochondrial biogenesis. Specifically, using an optimal nitric oxide donor supplementation, we showed a significant increase in urea, albumin secretion and intracellular albumin, cyp7A1 activity as compared to sodium butyrate treated hepatocyte-like cells. From a metabolic standpoint, highest mitochondrial mass and activity was observed in 500 μM SNAP treated cells as compared to "No SNAP" condition on day 15 of differentiation.

For future work, the utilization of mathematical programming techniques with the incorporation of extracellular metabolite measurements into a comprehensive metabolic reaction network model can be beneficial for identifying pathway flux differences between the different experimental conditions as compared to mature hepatocytes for possible metabolic engineering applications. Further, this methodology can be applied to ES cell differentiation systems involving metabolically active cells such as of the neuronal, pancreatic and cardiac lineages.

REFERENCES

1. Arias IM et al. The liver: biology and pathobiology. New York: Raven, 1994: 834.
2. Chan C, Berthiaume F, Nath BD et al. Hepatic tissue engineering for adjunct and temporary liver support: critical technologies. **Liver Transpl** 2004; 10(11):1331-42.
3. Yarmush ML, Toner M, Dunn JC et al. Hepatic tissue engineering. Development of critical technologies. **Ann N Y Acad Sci** 1992; 665:238-52.
4. Zandstra PW, Nagy A. Stem cell bioengineering. **Annu Rev Biomed Eng** 2004; 3:275-305.
5. Lavon N, Benvenisty N. Study of hepatocyte differentiation using embryonic stem cells. **J Cell Biochem** 2005; 96(6):1193-202.
6. Maguire T, Novik E, Schloss R et al. Alginate-PLL microencapsulation: effect on the differentiation of embryonic stem cells into hepatocytes. **Biotechnol Bioeng** 2006; 93(3):581-91.
7. Novik EI, Maguire TJ, Orlova K et al. Embryoid body-mediated differentiation of mouse embryonic stem cells along a hepatocyte lineage: insights from gene expression profiles. **Tissue Eng** 2006; 12(6):1515-25.
8. Sharma NS, Shikhanovich R, Schloss R et al. Sodium butyrate-treated embryonic stem cells yield hepatocyte-like cells expressing a glycolytic phenotype. **Biotechnol Bioeng** 2006; 94(6):1053-63.
9. Higuchi A, Kurihara M, Kobayashi K et al. Albumin and urea production by hepatocytes cultured on extracellular matrix proteins-conjugated poly (vinyl alcohol) membranes. **J Biomater Sci Polym Ed** 2005; 16(7):847-60.
10. Leary SC, Shoubridge EA. Mitochondrial biogenesis: which part of "NO" do we understand? **Bioessays** 2003; 25(6):538-41.
11. Nisoli E, Clementi E, Paolucci C et al. Mitochondrial biogenesis in mammals: the role of endogenous nitric oxide. **Science** 2003; 299(5608):896-9.
12. Nisoli E, Clementi E, Moncada S et al. Mitochondrial biogenesis as a cellular signaling framework. **Biochem Pharmacol** 2004; 67(1):1-15.
13. Bloch W, Fleischmann BK, Lorke DE et al. Nitric oxide synthase expression and role during cardiomyogenesis. **Cardiovasc Res** 1999; 43(3):675-84.
14. Magrinat G, Mason SN, Shami PJ et al. Nitric oxide modulation of human leukemia cell differentiation and gene expression. **Blood** 1992; 80(8):1880-4.

15. Peunova N, Enikolopov G. Nitric oxide triggers a switch to growth arrest during differentiation of neuronal cells. **Nature** 1995; 375(6526):68-73.

16. Davis RA, Miyake JH, Hui TY et al. Regulation of cholesterol-7alpha-hydroxylase: BARElyy missing a SHP. **J Lipid Res** 2002; 43(4):533-43.

17. Puigserver P, Adelmant G, Wu Z et al. Activation of PPARgamma coactivator-1 through transcription factor docking. **Science** 1999; 286(5443):1368-71.

18. Puigserver P, Spiegelman BM. Peroxisome proliferator-activated receptor-gamma coactivator 1 alpha (PGC-1 alpha): transcriptional coactivator and metabolic regulator. **Endocr Rev** 2003; 24(1):78-90.

19. Finck BN, Kelly DP. PGC-1 coactivators: inducible regulators of energy metabolism in health and disease. **J Clin Invest** 2006; 116(3):615-22.

20. Houten SM, Auwerx J. PGC-1alpha: turbocharging mitochondria. **Cell** 2004; 119(1):5-7.

21. Liang H, Ward WF. PGC-1alpha: a key regulator of energy metabolism. Adv Physiol Educ 2006; 30(4):145-51.

22. Lin J, Tarr PT, Yang R et al. PGC-1beta in the regulation of hepatic glucose and energy metabolism. **J Biol Chem** 2003; 278(33):30843-8.

23. Naiki T, Nagaki M, Shidoji Y et al. Analysis of gene expression profile induced by hepatocyte nuclear factor 4alpha in hepatoma cells using an oligonucleotide microarray. **J Biol Chem** 2002; 277(16):14011-9.

24. Puigserver P, Wu Z, Park CW et al. A cold-inducible coactivator of nuclear receptors linked to adaptive thermogenesis. **Cell** 1998; 92(6):829-39.

25. Yoon JC, Puigserver P, Chen G et al. Control of hepatic gluconeogenesis through the transcriptional coactivator PGC-1. **Nature** 2001; 413(6852):131-8.

26. Duncan SA. Transcriptional regulation of liver development. **Dev Dyn** 2000; 219(2):131-42.

27. Kanno S, Kim PK, Sallam K et al. Nitric oxide facilitates cardiomyogenesis in mouse embryonic stem cells. **Proc Natl Acad Sci U S A** 2004; 101(33):12277-81.

28. Farghali H, Martinek J, Masek K. The amelioration of hepatocyte oxidative stress injury by nitric oxide released from S-nitroso-N-acetyl penicillamine: a study in immobilized perfused hepatocytes. **Methods Find Exp Clin Pharmacol** 1999; 21(6):395-402.

29. Kucera T, Canova NK, Farghali H et al. The morphological and immunocytochemical evaluation of primary rat hepatocytes undergoing spontaneous cell death: Modulation by the nitric oxide donor S-nitroso-N-acetylpenicillamine. **Biomed Pap Med Fac Univ Palacky Olomouc Czech Repub** 2006; 150(1):75-82.

30. Asahina K, Fujimori H, Shimizu-Saito K et al. Expression of the liver-specific gene Cyp7a1 reveals hepatic differentiation in embryoid bodies derived from mouse embryonic stem cells. **Genes Cells** 2004; 9(12):1297-308.

31. Massimi M, Lear SR, Huling SL et al. Cholesterol 7alpha-hydroxylase (CYP7A): patterns of messenger RNA expression during rat liver development. **Hepatology** 1998; 28(4):1064-72.

FIGURE LEGENDS

Figure 1: Metabolic analysis of differentiated ES cells. (A) Glucose consumption rate (B) Lactate production rate. Data is normalized to Day 13 "No SNAP" condition.
**** indicates p < 0.05, ** indicates p < 0.001 vs. the same experimental condition on day 13 of differentiation.***

Figure 2: Evaluation of mitochondrial parameters. (A) Microscopic evaluation of Mitochondrial Mass and Activity (B) Percentage of NAO positive cells and (C) Percentage of cells with high mitochondrial activity. N-Acridine Orange (NAO), 5,5',6,6'-tetrachloro-1,1',3,3' tetraethylbenzimidazolylcarbocyanine iodide/chloride (JC-1).
**** indicates p < 0.05, ** indicates p < 0.001 vs. the no supplementation condition on the same day.***

Figure 3: Dynamic profile of hepatocyte-specific function for differentiated ES cells on days 13 and 15 of differentiation for different concentrations of SNAP. (A) Urea secretion rate (B) Albumin secretion rate. The data correspond to three independent experiments. * *indicates p < 0.05 vs. the no supplementation condition on the same day.*

Figure 4: Intracellular evaluation of albumin function. (A) Intracellular Albumin content (B) Percentage of Albumin positive cells on day 13 and 15 of differentiation. The data is representative of three independent experiments. * *indicates p < 0.05 vs. the no supplementation condition on the same day.*

Figure 5: Cytochrome P450 7A1 promoter activity on day 15 of differentiation. The data is normalized to the cytomegalovirus promoter activity for the experimental condition and is representative of three independent experiments. * *indicates p < 0.05 vs. the no supplementation condition.*

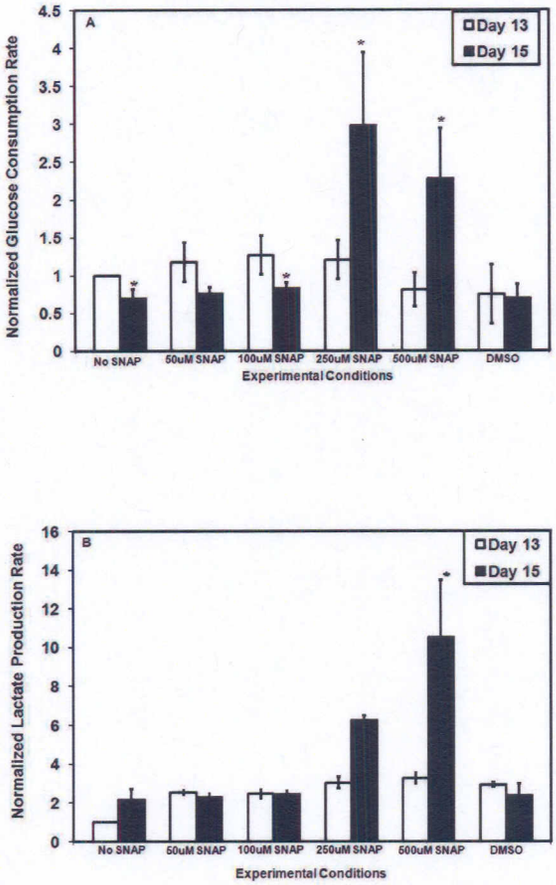

Figure 1: Metabolic analysis of differentiated ES cells. (A) Glucose consumption rate (B) Lactate production rate. Data is normalized to Day 13 "No SNAP" condition. * indicates p < 0.05, ** indicates p < 0.001 vs. the same experimental condition on day 13 of differentiation.

316x444mm (96 x 96 DPI)

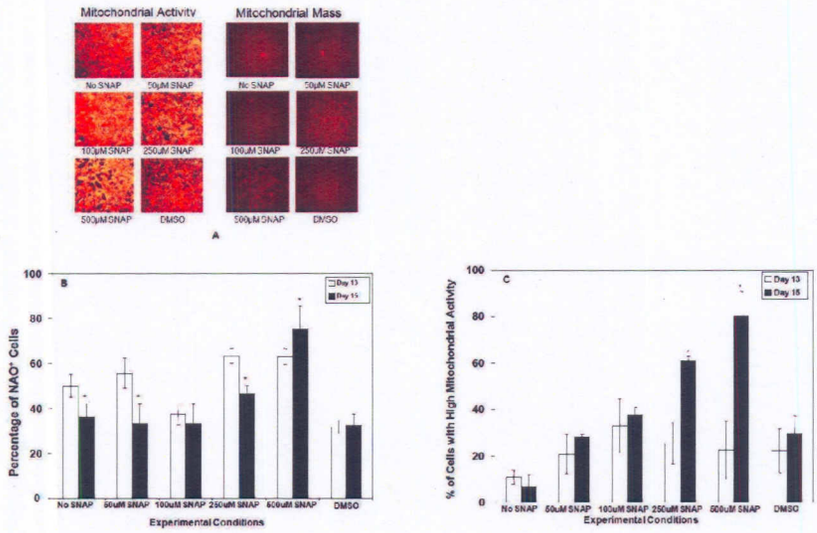

Figure 2: Evaluation of mitochondrial parameters. (A) Microscopic evaluation of Mitochondrial Mass and Activity (B) Percentage of NAO positive cells and (C) Percentage of cells with high mitochondrial activity. N-Acridine Orange (NAO), 5,5',6,6'-tetrachloro-1,1',3,3' tetraethylbenzimidazolylcarbocyanine iodide/chloride (JC-1). * indicates $p < 0.05$, ** indicates $p < 0.001$ vs. the no supplementation condition on the same day.
488x373mm (96 x 96 DPI)

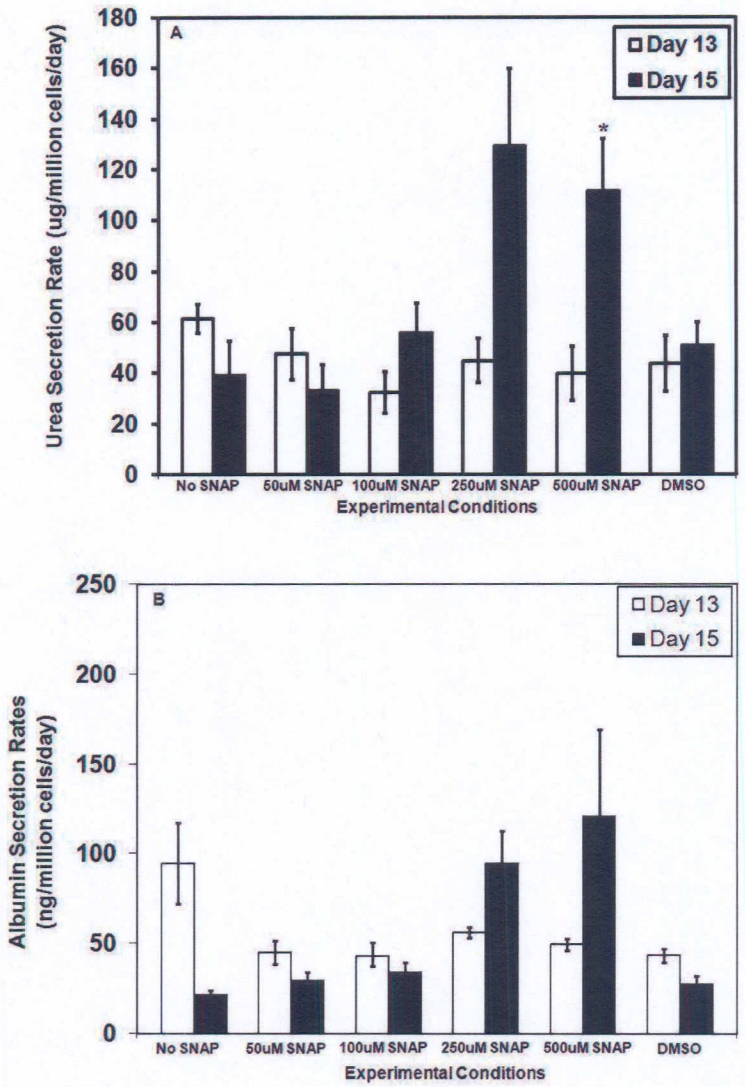

Figure 3: Dynamic profile of hepatocyte-specific function for differentiated ES cells on days 13 and 15 of differentiation for different concentrations of SNAP. (A) Urea secretion rate (B) Albumin secretion rate. The data correspond to three independent experiments. * indicates $p < 0.05$ vs. the no supplementation condition on the same day.
238x334mm (96 x 96 DPI)

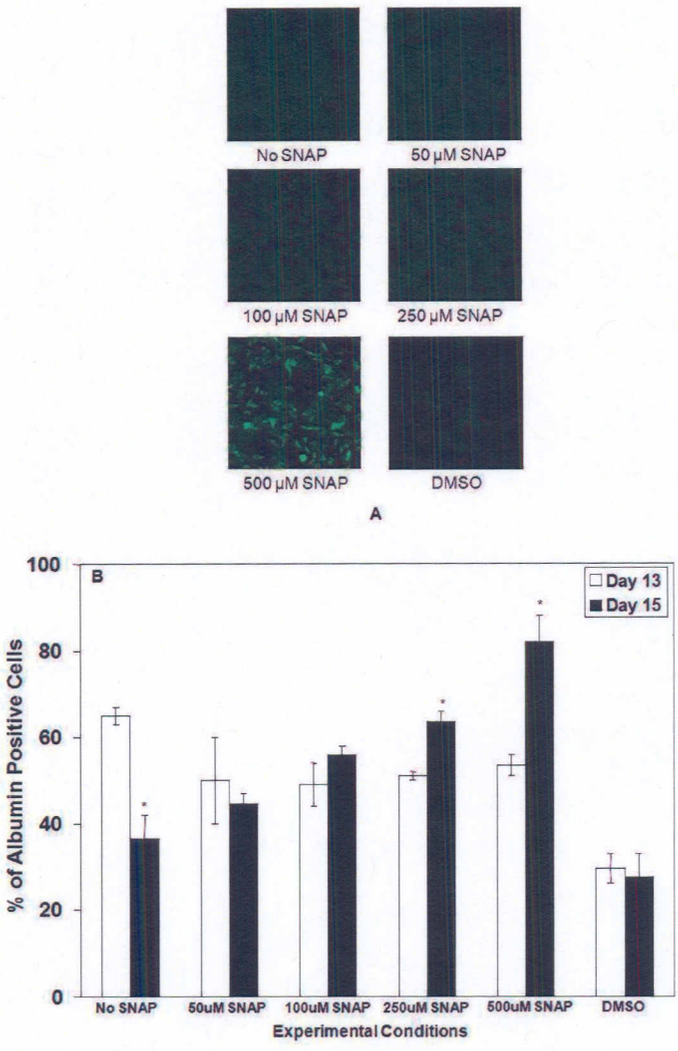

Figure 4: Intracellular evaluation of albumin function. (A) Intracellular Albumin content (B) Percentage of Albumin positive cells on day 13 and 15 of differentiation. The data is representative of three independent experiments. * indicates $p < 0.05$ vs. the no supplementation condition on the same day.

269x344mm (96 x 96 DPI)

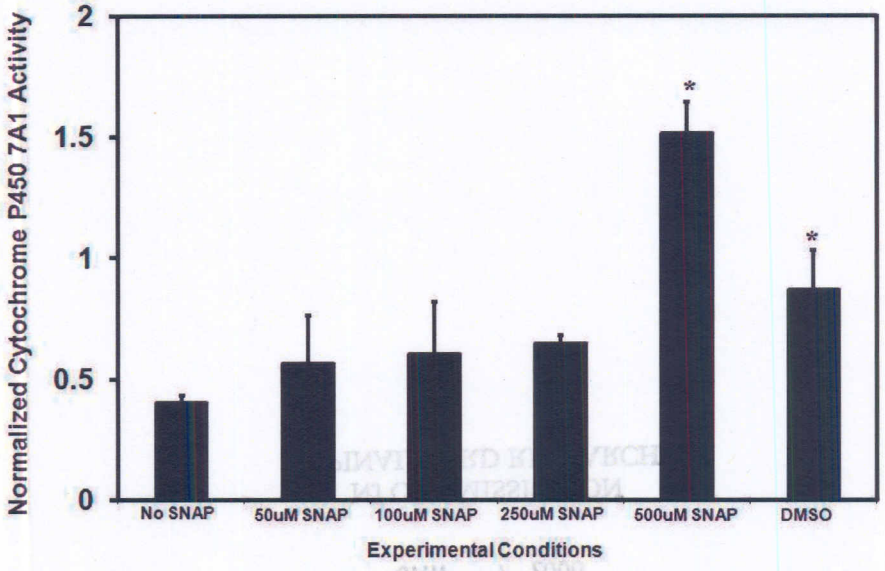

Figure 5: Dynamic profile of hepatocyte-specific function for differentiated ES cells on days 13 and 15 of differentiation for different concentrations of SNAP. (A) Urea secretion rate (B) Albumin secretion rate. The data correspond to three independent experiments. * indicates p < 0.05 vs. the no supplementation condition on the same day.

238x169mm (96 x 96 DPI)